RESEARCH PAPER

Bimetallic AuCu nanoparticles supported on CeO_2 as selective catalysts for glycerol conversion to lactic acid in aqueous basic medium

Ruben Palacio · Diana López · Diana Hernández

Abstract Gold-based catalysts, monometallic Au/CeO_2 or bimetallic AuCu/CeO_2, evaluated on the glycerol conversion to lactic acid, demonstrated to be active and selective at a reaction temperature of 220 °C in aqueous basic medium at low base concentration. The concentration of NaOH slightly modified the activity of AuCu/CeO_2 for converting glycerol, while selectivity toward lactic acid increased on AuCu/CeO_2 catalyst but had no influence on Au/CeO_2 catalytic performance. Recyclability tests demonstrated that AuCu/CeO_2 kept high conversion for up to the fourth catalytic cycle and selectivity remained stable, while conversion on Au/CeO_2 significantly decreased in the second cycle. For instance, copper stabilized gold on AuCu/CeO_2 catalysts for converting glycerol to lactic acid in aqueous medium at relatively high temperature of 220 °C. Characterization of AuCu/CeO_2 catalyst using H_2-TPR showed that the presence of Au modified the reduction events of Cu species, while HRTEM analysis of nanoparticles showed particles of an average size of 6.3 nm and lattice fringes for metallic Au and Cu. These results suggest that Au and Cu might be in close proximity.

R. Palacio (✉) · D. López · D. Hernández
Química de Recursos Energéticos y Medio Ambiente, Instituto de Química, Facultad de Ciencias Exactas y Naturales, Universidad de Antioquia UdeA, Calle 70 No. 52-21, Medellín, Colombia
e-mail: ralberto.palacio@udea.edu.co

Introduction

Glycerin is a byproduct obtained during transesterification reactions to produce biodiesel; it is generated in up to 10 wt% in the final mixture of the products (Monteiro et al. 2018). Glycerin formation is a downside in the industrial biodiesel production generating a surplus of glycerol in the global market. Selectively converting glycerin (crude glycerol) or glycerol (1,2,3-propanetriol) into valuable oxygenated chemical compounds is interesting for economical, industrial, and basic research (Behr et al. 2008; Johnson and Taconi 2007; Pagliaro et al. 2007; Ramírez-López et al. 2010; Zhou et al. 2008). Despite the recent global concerns and skepticism about biodiesel production and consequences in its utilization as fuel, the continuous increase in the worldwide production of biodiesel will continue in the next decade (Dodekatos et al. 2018); biodiesel reached an estimated 30.8 million m^3 production in 2016, thus generating roughly 3.08 million m^3 of crude glycerol (Anand and Saxena 2012; Monteiro et al. 2018). The high cost for purification of crude glycerol creates new needs for finding practical applications, one being its chemical transformation into added value and renewable chemical products. Among the wide variety of chemicals that can be obtained from glycerol, lactic acid is of significant importance because it is considered as one of the top chemical platforms (Bozell and Petersen 2010; Werpy et al. 2004), from which valuable industrial

oxygenates can be synthesized, such as acrylic and pyruvic acids, 1,2-propanediol, acrylate esters, or polylactic acid (Auneau et al. 2012; Bozell and Petersen 2010; Castillo Martinez et al. 2013; Datta and Henry 2006; Dusselier et al. 2013; Fan et al. 2009; Katryniok et al. 2013; Mäki-Arvela et al. 2014; Pereira et al. 2011).

Glycerol conversion to lactic acid was initially reported under hydrothermal conditions at high temperatures (250–300 °C) and high base to glycerol molar ratios (Hisanori Kishida 2005; Ramírez-López et al. 2010; Shen et al. 2009). Recently, homogeneous catalysts have been reported as an alternative to the harsh reaction conditions used during the hydrothermal conversion, leading to the production of lactic acid and also, hydrogen can be obtained (Li et al. 2015; Lu et al. 2016; Sharninghausen et al. 2014). Using different Ir complexes at 115 °C with 1.1 KOH equivalent with respect to glycerol during 24 h under N_2 atmosphere led to a maximum conversion of 94% with a selectivity of 97%, but still high concentration of base and long reaction times were needed to obtain a satisfactory catalyst performance (Sharninghausen et al. 2014). Using Ru complexes at 140 °C with 1.08 NaOH equivalent (6.0 M) led to a complete conversion of glycerol with a lactic acid yield of 62% (Li et al. 2015). Ir or Ru complexes bearing alkyl- and arylsulfonate-functionalized N-heterocyclic carbene were active for glycerol selective conversion to lactic acid at 150 °C in aqueous basic medium, using KOH (Finn et al. 2018). In general, Ir complexes showed higher activity than Ru complexes, and the best catalytic performance was observed for a catalyst containing Ir(I), with a TOF reaching 42,592 h^{-1} and heating under microwave radiation for 3 h, while under conventional heating a TOF of 3477 h^{-1} was obtained. The catalyst showed a comparable activity using crude glycerol. On the other hand, Ir-prydine-carbene complexes demonstrated to be active for neat glycerol conversion to lactate (Lu et al. 2016). The best catalyst of the prepared series of complexes showed a TOF of 4×10^4 h^{-1} at 145 °C within the first hour reaction time, besides the catalyst was tolerant to some strong poison compounds.

The use of heterogeneous catalysts has also been proposed for transforming glycerol into lactic acid. Noble metal-based catalysts were among the first used, monometallic or bimetallic particles were dispersed on supports of different chemical nature and reaction was performed under different reaction conditions (see Table 3 for additional information in the results and discussion section). Monometallic Pt (Maris and Davis 2007) or bimetallic PtRu and AuRu (Maris et al. 2007) catalysts, using carbon as an inert support, led to a selectivity toward lactic acid of 60–62% at 20–21% glycerol conversion at 200 °C with a NaOH/glycerol molar ratio around 7.36 and under 40 bar of H_2 pressure. Platinum supported on a basic support, Pt/CaCO$_3$, allowed to obtain a 46% glycerol conversion, with a 56% lactic acid selectivity at 200 °C, pH 12, and in presence of boric acid and H_2 (ten Dam et al. 2011); however, under N_2 atmosphere, a 86% glycerol conversion with a 58% lactic acid selectivity was obtained. In contrast, platinum supported on reducible titanium or zirconium oxides reached higher selectivity to lactic acid, 83–84%, at higher glycerol conversion of 76% on Pt/TiO$_2$ and 95% on Pt/ZrO$_2$, reaction performed at 180 °C with a NaOH/glycerol molar ratio of 1.8, 40 bar He pressure and 24 h reaction (Ftouni et al. 2015). Iridium supported on an inert support, Ir/C, also demonstrated to be active in glycerol conversion to lactic acid (Auneau et al. 2012; Auneau et al. 2011). Ir/C in alkaline medium (1 M NaOH) at 180 °C produced 1,2-propanediol and lactic acid, the yield depending on the atmosphere of the reaction (inert He or reducing H_2). Rh/ZnO catalyst in alkaline medium and under H_2 atmosphere at 200 °C, under 20 bar of H_2, led to 68% selectivity toward lactic acid at ~ 100% glycerol conversion (Checa et al. 2012).

Non-noble metal oxides or metallic particles have also been reported as active phases for converting glycerol into lactic acid at high copper or cobalt loadings (Palacio et al. 2018a; Palacio et al. 2018b; Roy et al. 2011; Yang et al. 2016; Yin et al. 2016). Copper-based catalysts demonstrated to be active for activating glycerol toward lactic acid formation at 240 °C, under 14 bar of N_2 pressure with NaOH to glycerol molar ratio of 1.1 (Roy et al. 2011). Lactic acid selectivity reached 78–80%, although conversion was dependent on the chemical nature of the support, reaching 75% over silica and 98% over Al$_2$O$_3$ (Roy et al. 2011). Metallic copper has been supported on MgO, ZrO$_2$, and hydroxyapatite (HAP) (Yin et al. 2016), with Cu/HAP exhibiting a selectivity toward lactic acid of 90% at 91% glycerol conversion (reaction performed at 230 °C and under N_2 atmosphere). More recently, it has been reported that CuO/CeO$_2$ catalyst led to a 74.4% lactic acid selectivity at 87.3% conversion of glycerol at 220 °C, under N_2 atmosphere at 8 h reaction and a NaOH to glycerol molar ratio of 1.0, with catalyst showing high stability

(Palacio et al. 2018b). At low copper loadings, copper promoted with palladium supported on reduced graphene oxide (CuPd/rGO) led to a 53.1% glycerol conversion at 16 h reaction with a lactic acid selectivity around 85.6% (reaction performed at 140 °C, 1.4 MPa of N_2, with NaOH to glycerol molar ratio of 1.1) (Jin et al. 2013). On the other hand, cobalt oxide supported on CeO_2, Co_3O_4/CeO_2, demonstrated activity in glycerol selective conversion to lactic acid (250 °C and 60 bar of N_2) (Palacio et al. 2018a). Glycerol conversion reached more than 70% at 8-h reaction time, while selectivity toward lactic acid reached 79.8% depending on the preparation method of the catalyst, but the catalysts showed poor stability under the reaction conditions. However, a drawback of copper- and cobalt-based catalysts is that they are active at high metal loadings, in general 15 wt% to 35 wt%.

In recent decades, heterogeneous gold-based catalysts have gained attention because at the nanoscale, gold species are active in a wide number of reactions, including glycerol activation to produce different oxygenated molecules (Haruta 2014; Hutchings and Haruta 2005; Prati and Rossi 1998; Shen et al. 2010; Zope et al. 2010). AuCu/CeO_2 materials have well-known oxidation properties (Ma et al. 2017; Wilson et al. 2015). Supported AuCu catalysts have demonstrated activity for alcohol oxidation, among which glycerol has also been studied (Della Pina et al. 2008; Sobczak and Wolski 2015). However, lactic acid production from glycerol on AuCu-based catalysts is scarcely reported. Unsupported bimetallic AuCu nanoparticles, with different Cu/Au ratios showed activity in glycerol selective conversion to lactic acid using high catalyst loading (reaction performed at 200 °C, 100 mL of aqueous solution with a NaOH/glycerol molar ratio of 1.1 and 0.736 g of catalyst for 2 h) (Shen et al. 2017), conversion of glycerol reaching more than 99% with a lactic acid selectivity higher than 93.8%. Activity of catalyst $AuCu_2$ remained high after 6 catalytic cycles, demonstrating a high stability of the bimetallic nanoparticles under the reaction conditions. For instance, studies with supported AuCu nanoparticles are interesting for evaluating the potential of such catalysts for obtaining lactic acid from glycerol.

In this work, Au and Cu were selected as active phases because both have shown activity for converting glycerol to lactic acid, copper species are active only at high loadings (> 10 wt%) and can lead to the production of hydrogen during lactic acid formation; for instance, in

this work, we studied its potential at lower loading combined with gold for obtaining bimetallic AuCu nanoparticles stabilized in CeO_2 support. Au species are not stable under different reaction conditions, thus combining Au with Cu could result in improving stability of gold and modified surface properties (Liu et al. 2008b; Wilson et al. 2015), favoring selectivity toward lactic acid and hydrogen formation from glycerol. CeO_2 was selected as support because it has been reported in some of our previous research publications (Palacio et al. 2018b) that it is not active for converting glycerol to lactic acid and besides; it is stable under the selected catalytic reaction conditions which have demonstrated that copper oxide is stabilized on cerium oxide avoiding leaching. Under the catalytic reaction conditions, Au/CeO_2 and AuCu/CeO_2 catalysts are both active and selective for converting glycerol into lactic acid under inert atmosphere in alkaline media. The presence of copper improves recyclability and stability in ceria supported gold-based catalyst.

Experimental section

Preparation of CeO_2 support

27.09 g of Ce $(NO_3)_3 \cdot 6H_2O$ and 57.8 g of NaOH are mixed in 720 mL of ultrapure H_2O, and the resulting mixture is stirred during 15 min at 20 °C. Thereafter, the resulting solution is transferred into a teflon-lined stainless-steel autoclave, sealed and placed in an oven at 100 °C for 14 h. The precipitate is recovered by filtration, washed with ultrapure H_2O, and dried at 90 °C for 24 h.

AuCu/CeO_2 composite preparation

Following a similar procedure as described in previous works (Chang et al. 2009; Haruta 1997), 2.75 mL of a $HAuCl_4 \cdot 3H_2O$ solution (containing 1 g of $HAuCl_4 \cdot 3H_2O$ in 50 mL solution, with ultrapure water) is mixed with 40 mL ultrapure water under magnetic stirring at room temperature (around 20 °C). Then, 0.11 g of Cu $(NO_3)_2 \cdot 3H_2O$ (nominal Cu loading of 1 wt%) is added under magnetic stirring. The temperature is then increased to 60 °C and the pH raised to 9.0 by dropwise addition of a 0.1 M NaOH solution. After pH and temperature both stabilized at the target values, 3.0 g of as-synthesized CeO_2 powder is added and the

magnetic stirring is continued for 4 h at 60 °C, keeping the pH at 9.0. The powder is recovered by filtration and washed with ultrapure water, dried at 60 °C for 72 h under vacuum, and further calcined at 400 °C during 4 h in a muffle oven (temperature rate of 2 °C min^{-1}). Samples were prepared containing Cu or Au following similar conditions as previously described. The samples are denoted as: *Cu/CeO$_2$*, *Au/CeO$_2$*, and *AuCu/CeO$_2$*.

Characterization of supports and catalysts

Atomic absorption spectroscopy was used to determine the copper and gold loadings, using a Thermo instrument 3000-series instrument. For analysis, powders were dissolved in a solution of aqua regia containing HF during 12 h.

The specific surface area was determined using N$_2$-physisorptio at 77 K, on a Micromeritics ASAP 2020 instrument. The powders were heated under vacuum at 250 °C during 12 h before the analysis. The Brunauer-Emmett-Teller was applied to determine the specific surface area, for P/P_0 range of 0.05 to 0.35.

Scanning electron microscopy (SEM) images were obtained using a JEOL JSM-6490 LV instrument. For analysis, the powders were deposited on a graphite ribbon. The microscope is equipped with an EDX analyzer, allowing performing element mapping.

High-resolution transmission electron microscopy (HRTEM) images were recorded on a Tecnai F20 Super Twin TMP instrument. The powders were dispersed in ethanol and sonicated for 30 min and then dropped on a carbon-coated nickel grid for analysis.

Temperature programmed reduction (TPR) analysis was carried out in an AUTOCHEM2010 Micromeritics. For analysis, 120 mg of powder was placed in a U-tube and treated under Ar flow (50 mL min^{-1}, ramp of 5 °C min^{-1}) at 400 °C during 60 min. Then, the temperature was adjusted to 50 °C, and the powder was finally heated from 50 °C to 900 °C (ramp of 10 °C min^{-1}) under H$_2$ flow (10 vol% diluted in Ar, 50 mL min^{-1}).

Catalytic tests

Evaluation of the catalytic properties of the catalysts is conducted in a 250 mL batch Parr reactor autoclave (Palacio et al. 2018b). One hundred twenty milliliters of 0.47 M aqueous NaOH solution and 7.67 g of glycerol solution (85 wt%) are mixed into the autoclave (NaOH to glycerol (GLY), NaOH/GLY, molar ratio is

0.8). Six hundred milligrams of catalyst were then added, and the autoclave was sealed, flushed with N$_2$, and heated up under autogenous pressure until the reaction temperature, 220 °C. The increasing temperature from ambient temperature to 220 °C took 40 min on average. Once the temperature of the autoclave reached 220 °C, the pressure is immediately adjusted with 42 bar of N$_2$, and the stirring settled to 650 rpm (initial time for reaction, t_o). After 8 h reaction, the reaction mixture was analyzed by taking 0.35 mL of the solution and quenched with 1.0 mL H$_2$SO$_4$ aqueous solution (0.5 M). Isopropanol was added as internal standard (0.05 mL). Sample was then filtered, and reaction products were analyzed by using liquid chromatography (Agilent 1200 series chromatograph using a refractive index (RI) detector, equipped with an ICSep ICE-COREGEL-87H3 column—mobile phase 0.005 M H$_2$SO$_4$, flow 0.5 mL min^{-1}—T_{column} = 70 °C). Additionally, the gas phase was analyzed by using gas chromatography, using an Agilent Technologies instrument model 6890 N, equipped with a TCD and a FID detector, using a Carboxen 1010 PLOT fused silica capillary column (30 m × 0.53 mm) and an Agilent DB-PETRO column (50 m length, 0.2 mm diameter).

The conversion of glycerol is calculated according to the following equation:

$$C_{GLY}(\%) = \left(\left(n_{GLY,in} - n_{GLY,out} \right) / n_{GLY,in} \right) x\ 100 \qquad (1)$$

where $n_{GLY,in}$ and $n_{GLY,out}$ are the GLY initial amount and the residual GLY amount at time t, respectively.

The product selectivity is calculated according to the following equation:

$$S_i(\%) = \left(n_i / \left(n_{GLY,in} - n_{GLY,out} \right) \right) x\ 100 \qquad (2)$$

where n_i represents the number of moles of product i formed.

Carbon balance is determined according to the following equation:

$$C_{balance}(\%) = \left(\Sigma n_{C\ product\ i} + n_{C\ GLY,out} \right) / n_{C\ GLY,in} \right) \times 100 \qquad (3)$$

where $n_{C\ product\ i}$ represents the number of mole of carbon (C) in product i formed and $n_{C\ GLY,in}$ and $n_{C\ GLY,out}$ represents the number of mole of carbon (C) in the initial amount of glycerol and the number of mole of carbon (C) in residual GLY amount at time t, respectively.

Results and discussion

Catalyst characterization

The metal loading is determined using atomic absorption and the results showed the copper metal content reached the nominal one (1 wt%) in both monometallic and bimetallic composites (Table 1), while gold loading is slightly lower than the expected one (Table 1). These results indicated a successful deposition of gold and copper species in both monometallic and bimetallic composites. Besides, the copper and gold loadings are similar between both composites, which is important because differences in physicochemical properties or reactivity cannot be attributed to a different loading of the active phases in the catalytic materials.

The specific surface area for CeO_2 support is $122 \ m^2 \ g^{-1}$ and after copper, gold, or gold-copper species deposition, the values remained close to the value for the parent support, $114–131 \ m^2 \ g^{-1}$ (Table 1). The CeO_2 support shows a type IV isotherm with a wide pore size distribution (Fig. S1) and even after deposition of 5.7 wt% of copper, the isotherm and pore size distribution do not show significant changes; thus, the deposition of gold and copper do not modify the textural properties of the support. These results suggest the monometallic or bimetallic metal species are well-distributed on the CeO_2 support surface; thus, the different composites exhibit a high specific surface area.

SEM images after copper, gold, or gold-copper deposition (Fig. S2) showed that the powder contains amorphous and aggregated particles of CeO_2, without a well-defined particle shape and size (Palacio et al. 2018b). SEM-EDX characterization of Cu/CeO_2 and Au/CeO_2 composites after reduction of the calcined powder at 400 °C (Fig. 1) indicated that both copper and gold species are observed all around the area analyzed, thus showing a rather homogeneous distribution on the CeO_2 support. For $AuCu/CeO_2$ composite (Fig. 2), Au species are well distributed on the composite, indicating that the presence of copper does not modify distribution of gold species. In the case of copper, the species are observed all around the analyzed area (Fig. 2b, d, f); however, the intensity of the copper signal appeared more intense in some areas suggesting that copper slightly agglomerated during calcination and reduction steps at 400 °C.

HRTEM characterization of the $AuCu/CeO_2$ composite after reduction of the calcined powder at 400 °C (Fig. 3) shows few small particles on the CeO_2 surface, with a particle size distribution centered at 6.3 nm. Consequently, these results might suggest a high distribution of small sized nanoparticles of AuCu on CeO_2 support. The length of the fringes measured on these nanoparticles, mainly 0.16 and 0.2 nm, are close to the reported for (i) cubic Cu: Cu(111), Cu(002) planes (Fiche 98-005-3755), and (ii) cubic Au: Au(002) planes (Fiche 98-004-4362). For instance, in agreement with TPR characterization (see results below), gold and copper might be in close proximity and interaction between both species is possible. In the case of Au/CeO_2 composite, particles were even more difficult to observe (not shown). TEM images showed that CeO_2 is composed of aggregated amorphous particles and in some extend by nanorods (Fig. 3). However, that rod-like shaped CeO_2 particles were observed only in few areas of the analyzed powder. The characterization of textural and morphological properties indicated that CeO_2 support together with the deposition-precipitation method, allowed to disperse tiny gold-copper species in the composites.

The TPR profile of CeO_2 support shows two main signals for hydrogen consumption in the temperature range of 200 to 850 °C (Fig. 4), in agreement with previous published results (Cargnello et al. 2010; Liu et al. 2008a; Zhang et al. 2014). The reduction peak at 448 °C has been attributed to the reduction of surface oxygen species on CeO_2, and the shoulder at 340 °C attributed to the formation of non-stoichiometric CeO_x oxides (Zhang et al. 2014). The reduction peak at 721 °C is commonly attributed to the reduction of bulk oxygen species. The lower temperature reduction peak for CeO_2 powder is not observed after Cu, Au, or AuCu species deposition, therefore indicating that the presence of these metal species modified the reduction properties of the CeO_2 support. The TPR profiles of Au/CeO_2 and

Table 1 Loading of gold and copper and textural properties of Au/CeO_2, Cu/CeO_2, and $AuCu/CeO_2$ composites

Composite	Au and Cu loading (wt%)		S_{BET} ($m^2 \ g^{-1}$)
	Au	Cu	
CeO_2	–	–	122
Au/CeO_2	0.7	–	131
Cu/CeO_2	–	1.0	123
$AuCu/CeO_2$	0.8	1.0	114

Fig. 1 EDX-mapping analysis of **a**, **b** Cu/CeO_2 and **c**, **d** Au/CeO_2 composites after reduction at 400 °C of the calcined powder
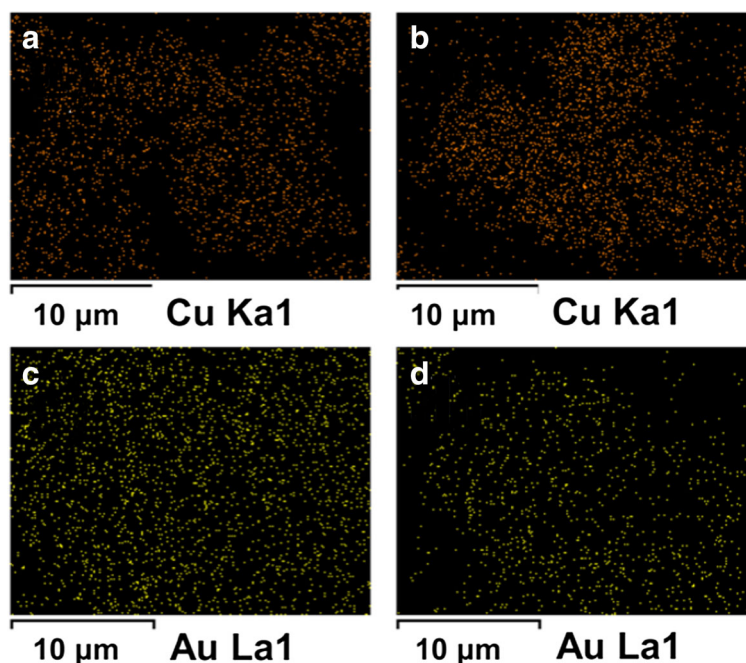
$AuCu/CeO_2$ composites only showed one reduction step at low temperature. For Au/CeO_2, the reduction peak is observed at 104 °C. This peak has been correlated to (i) a decrease in the reduction temperature of surface oxygen species of CeO_2, indicating that the presence of Au modified CeO_2 reduction properties (Liu et al. 2012; Si and Flytzani-Stephanopoulos 2008; Zhang et al. 2014), because of gold species strongly bounded on CeO_2 surface weaken the Ce-O bond, and (ii) reduction of Au^{n+} species. The TPR profile of Cu/CeO_2 composite on the other hand exhibited two major signals at temperatures lower than 300 °C. The lower temperature reduction peak at 142 °C might indicate, as observed for Au/CeO_2, a decrease in the reduction temperature of surface oxygen species of CeO_2; the peak at higher reduction temperature of 186 °C can be attributed to the reduction of clusters of oxidized copper species. In the case of $AuCu/CeO_2$, only one reduction peak is observed at low temperature, centered at lower reduction temperature than for Au/CeO_2 (78 °C), indicating as in the case of Au/CeO_2 a modification of the reduction properties of surface oxygen species on CeO_2 because of the presence of Au and Cu species on the surface. Additionally, the reduction step of oxidized copper species is not observed on the $AuCu/CeO_2$ composite, suggesting that interaction between Au and Cu led to the formation of reduced copper species. Consequently, the presence of Au species modified the chemical

properties of CuO_x species on the CeO_2 surface and suggested a possible close interaction between gold and copper species, generating AuCu species with copper in a reduced state (Cu^0) in the composite.

Catalytic reaction

The catalytic tests were performed for 8 h, such time being a good compromise between conversion and selectivity toward the target product, lactic acid (Palacio et al. 2018b). As a first remark, carbon balance approaches 98% indicating that adsorption on catalyst surface or carbon containing byproducts in the gas phase remained negligible under the catalytic reaction conditions. As a matter of fact, the analysis of the gas phase using gas chromatography allowed the identification of hydrogen gas, thus during the formation of lactic acid from glycerol hydrogen is also produced.

The glycerol conversion at 8 h reaction in N_2 atmosphere at 220 °C reached 18.8% without catalyst and with a NaOH to glycerol molar ratio of 0.8, while in presence of CeO_2 support, reached 20% (Table 2). For instance, there is not significant influence of the CeO_2 support on the conversion of glycerol under the catalytic reaction conditions. In presence of Cu/CeO_2 catalyst, the glycerol conversion reached 20.1%; therefore, the presence of copper at low loadings does not show catalytic activity. It has been reported

Fig. 2 EDX-mapping analysis of AuCu/CeO$_2$ composite after reduction at 400 °C of the calcined powder for **a**, **c**, **e** gold species and **b**, **d**, **f** copper species
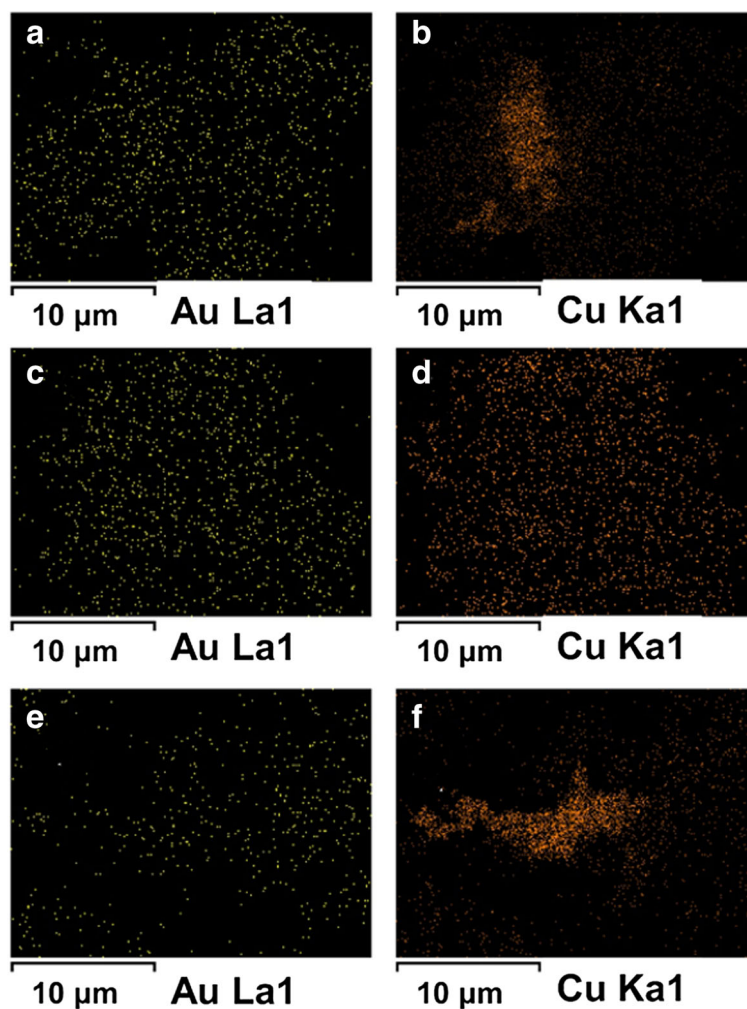
that unsupported or supported copper oxides or metal copper species on different supports are active at high copper loadings (Palacio et al. 2018b; Roy et al. 2011; Yang et al. 2016; Yin et al. 2016). The presence of copper slightly modifies selectivity toward lactic acid and pyruvaldehyde when compared to the reaction performed without catalyst or in presence of CeO$_2$ support. On Au/CeO$_2$ catalyst, the glycerol conversion reached 74.5% while when using AuCu/CeO$_2$ catalyst reached 70.2% (Table 2). These

Fig. 3 HRTEM images for AuCu/CeO$_2$ sample after calcination at 400 °C and further reduction at 400 °C
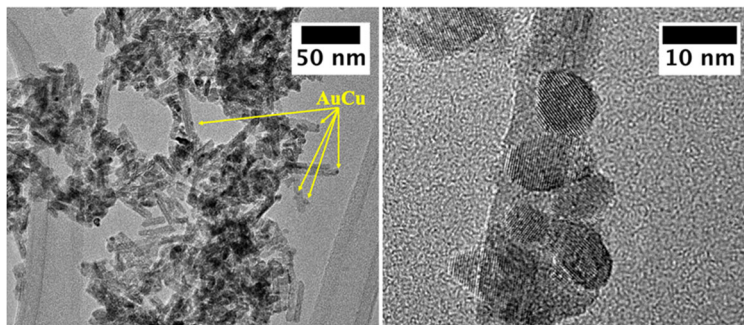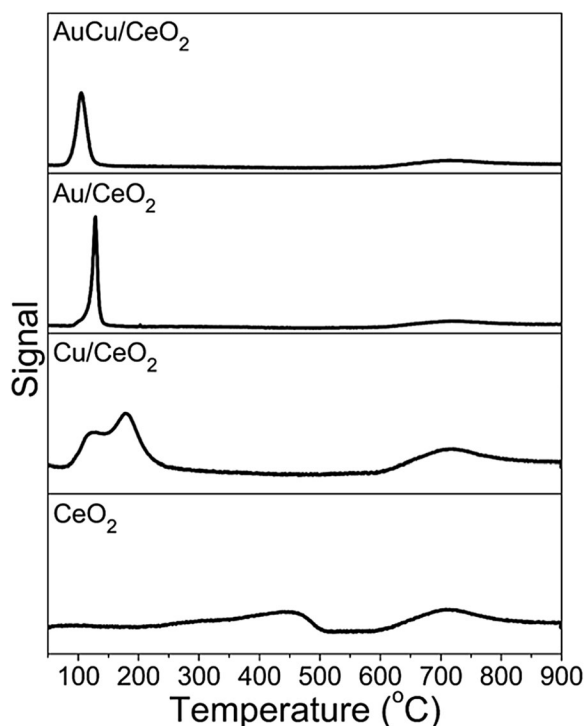
Fig. 4 TPR profiles of CeO$_2$ support, Cu/CeO$_2$, Au/CeO$_2$, and AuCu/CeO$_2$ composites after calcination at 400 °C

results indicate that gold species are active for adsorbing, activating, and thus converting glycerol under the catalytic reaction conditions, high temperature, and in basic aqueous medium, and are more than three times more active than copper species.

Lactic acid is the main product formed in presence of copper- or gold-based catalysts; however, selectivity with gold-based catalysts is higher and is slightly higher on Au/CeO$_2$ than on AuCu/CeO$_2$ catalyst, 92.4% and 87.5%, respectively. Increasing the reaction temperature to 250 °C on AuCu/CeO$_2$ catalyst resulted in an increase of glycerol conversion and a slightly decrease on the lactic acid selectivity, 87.2% and 76.5%, respectively. On the other hand, performing the reaction in presence of H$_2$ instead of N$_2$ decreased the glycerol conversion to 40.1% and selectivity toward lactic acid to 68%. Thus, reducing H$_2$ atmosphere is detrimental for the catalytic activity of AuCu/CeO$_2$ catalyst for converting glycerol into lactic acid while generating hydrogen gas. The high pressure of hydrogen gas since the beginning of the reaction inhibits the conversion of glycerol because it shifts the balance toward the reactive avoiding product formation. An increase in the NaOH concentration to 0.6 M, NaOH/GLY molar ratio equal to 1, at 220 °C and N$_2$ atmosphere, led to a slightly increase on the glycerol conversion with Au/CeO$_2$ catalyst while the increase was more important for AuCu/CeO$_2$ catalyst, from 70.2% with a NaOH/GLY of 0.8 to 77.8% with a NaOH/GLY of 1 (Table 2). Increasing the NaOH/GLY molar ratio to 1 did not modify selectivity toward lactic acid on Au/CeO$_2$ catalyst, while on AuCu/CeO$_2$ selectivity increased from 87.5 to 91.2%. Therefore, the presence of copper does not modify catalytic activity of the AuCu/CeO$_2$ catalyst, but the increase in NaOH concentration led to a better catalytic performance of the

Table 2 Catalyst reactivity at 220 °C

Catalyst	NaOH/GLY molar ratio	C_{GLY} (%)	Selectivity (%)					
			LA	1,2-PDO	PYR	GLA	AA	HDA
Without catalyst	0.8	18.8	14.2	0	14.4	0	0	0
CeO$_2$	0.8	20.0	13.9	0	14.5	0	0	0
Cu/CeO$_2$	0.8	20.1	20.3	0	17.8	1.8	0	0
Au/CeO$_2$	0.8	74.5	92.4	1.9	2.6	0	1.7	0.8
Au/CeO$_2$	1.0	75.5	92.6	1.9	2.6	0	1.9	1.0
AuCu/CeO$_2$	0.8	70.2	87.5	4.5	5.7	0	1.5	0.8
AuCu/CeO$_2$*	0.8	87.2	76.5	3.7	6.9	0	2.6	1.0
AuCu/CeO$_2$+	0.8	40.1	68	6	6.7	0	0	0
AuCu/CeO$_2$	1.0	77.8	91.2	2.4	3.8	0	2.1	0.4

GLY glycerol, *LA* lactic acid, *1,2-PDO* 1,2-propanediol, *PYR* pyruvaldehyde, *GLA* glyceraldehyde, *AA* acetic acid, *HDA* hidroacetone

*Reaction at 250 °C

+Reaction in presence of H$_2$ instead of N$_2$

Table 3 Catalytic results of different Au-, Pt-, Ru-, and Cu-based heterogeneous catalysts

Catalyst	Metal loading (wt%)	C_{GLY} (%)	S_{LA} (%)	NaOH/GLY	Atmosphere	T (°C)	Time (h)	Ref.
AuRu/C	Au: 0.85 Ru: 5	21	60	7.36	H_2/40 bar	200	5	Maris et al. 2007
PtRu/C	Pt: 1.9 Ru: 4.7	22	41	7.36	H_2/40 bar	200	5	Maris et al. 2007
$AuCu_2$ (bulk)	–	99	93.8	1.1	N_2	200	2	Shen et al. 2017
Pt/CaCO$_3$	Pt: 5			0.001	N_2/20 bar	200	18	ten Dam et al. 2011
Pt/TiO$_2$	Pt: 0.9	76	83	1.8	He/30 bar	180	24	Ftouni et al. 2015
Pt/ZrO$_2$	Pt: 1.2	94	84	1.8	He/30 bar	180	24	Ftouni et al. 2015
Cu/MgO	Cu: 16	99	83	1.1	N_2	230	8	Yin et al. 2016
Cu/ZrO$_2$	Cu: 16	64	50	1.1	N_2	230	8	Yin et al. 2016
Cu/HAP	Cu: 16	99	87	1.1	N_2	230	8	Yin et al. 2016
AuCu/CeO$_2$	Au: 0.8 Cu: 1.0	77.8	91.2	1	N_2/42 bar	220	8	a

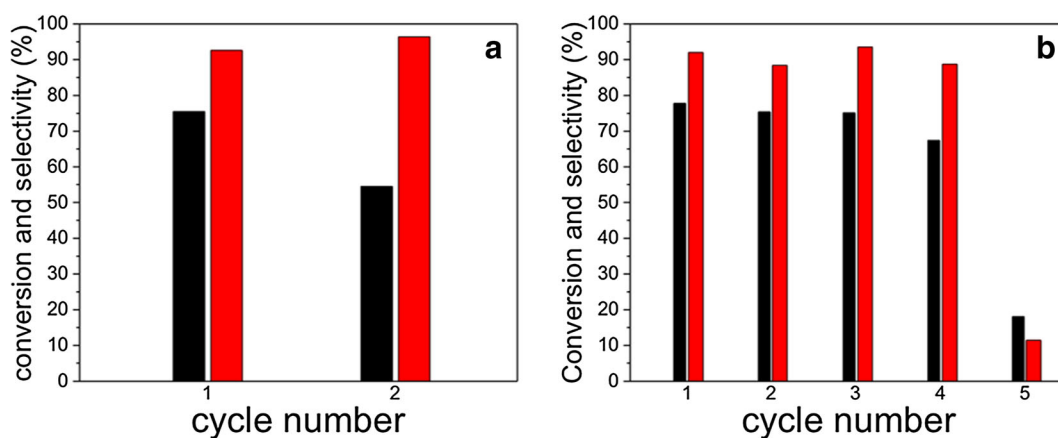*GLY* glycerol, *LA* lactic acid

[a] This work

AuCu/CeO$_2$ catalyst in terms of increasing glycerol conversion and lactic acid selectivity.

For comparison, a summary of representative results on glycerol conversion to lactic acid reported in the literature over noble metal- and copper-based heterogeneous catalysts is presented in Table 3. The catalytic results reported in this work are among the best in terms of moderate glycerol conversion with high selectivity toward lactic acid on bimetallic AuCu/CeO$_2$ catalyst. The high selectivity toward lactic acid is comparable to that reported for bulk AuCu$_2$ catalyst.

Stability of catalysts under the reaction conditions is studied by using recyclability tests which were performed for Au/CeO$_2$ and AuCu/CeO$_2$ catalysts. The powder was recovered by centrifugation and washed after the first catalytic cycle. Finally, the powders were dried and then calcined at 400 °C during 4 h. Before catalytic test, the catalysts were reduced at 400 °C. The reaction was performed adjusting the mass of glycerol to the mass of the recovered and calcined catalyst, keeping constant the NaOH/GLY mole ratio equal to 1.0 and the volume of the NaOH solution of 120 mL. The results show that on Au/CeO$_2$ catalyst (Fig. 5a), the glycerol conversion decreased from 75.5 to 54.5% in the second cycle while keeping a high selectivity toward lactic acid of 92.6–96.4%. A different

Fig. 5 Recyclability tests for **a** Au/CeO$_2$ catalyst and **b** AuCu/CeO$_2$ catalyst. Glycerol conversion (black bars) and selectivity to lactic acid (red bars)

Fig. 6 EDX-mapping analysis of AuCu/CeO$_2$ catalyst recovered after reaction: **a**, **b** copper species and **c**, **d** gold species
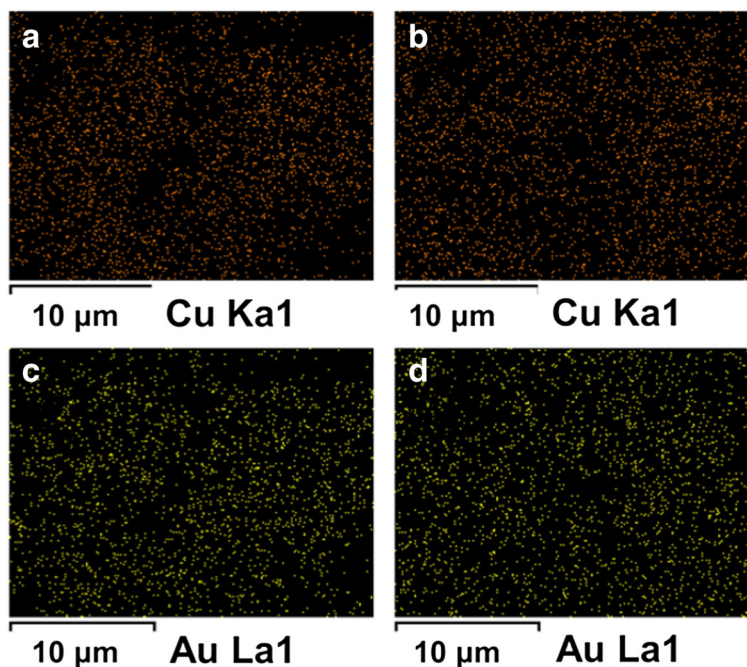
catalytic performance was observed on AuCu/CeO$_2$ catalyst (Fig. 5b); between 1st and 3rd cycle, the glycerol conversion remained in the range 75.1–77.8% with a high selectivity toward lactic acid in the range 88.4–93.5%. Thereafter, the glycerol conversion decreased to 67.4% in the 4th cycle but with a selectivity toward lactic acid of 88.7%. In the fifth cycle however, conversion only reached 18% and the lactic acid selectivity dropped down to 11.4%. Therefore, the presence of copper modifies the catalytic properties of gold in the

Fig. 7 EDX-mapping analysis of AuCu/CeO$_2$ catalyst after the fifth catalytic cycle (calcined and reduced at 400 °C): **a**, **b** copper species and **c**, **d** gold species
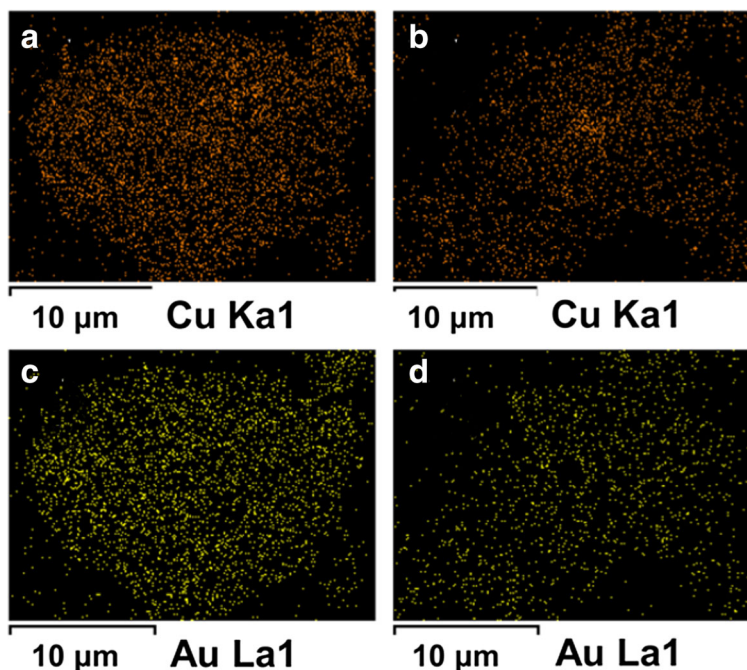
glycerol conversion to lactic acid, apparently increasing the stability of the active Au species. Reported studies on stability of Au-Cu have suggested that the formation of the alloy might modify the electronic structure of the nanoparticles and induce small particles formation, which are resistant to sintering (Liu et al. 2008b; Wilson et al. 2015). According to TPR and HRTEM characterization, copper and gold species might be in close proximity which increased stability of the catalysts.

Characterization of AuCu/CeO$_2$ catalyst after reaction

After the first catalytic reaction, the recovered AuCu/CeO$_2$ catalyst was analyzed by SEM-EDX (Fig. 6). SEM-EDX characterization indicated that copper and gold species are identified and observed all around the area analyzed indicating a rather homogeneous distribution on the CeO$_2$ support. For instance, during the reaction, the catalyst is not apparently modified and CeO$_2$ kept homogeneous distributed and stabilized copper and gold species.

The catalyst was also characterized after the fifth catalytic cycle. The powder was recovered, washed, dried, and calcined at 400 °C. The metal loading is determined using atomic absorption and the results showed that gold metal content decreased to 0.3 wt%. Thus, the low catalytic activity reached in the 5th catalytic cycle might be attributed to the leaching of gold, reaching a 0.3 wt% instead of the 0.7 wt% determined in the fresh catalyst. Characterization of the powder after calcination and further reduction at 400 °C by SEM-EDX (Fig. 7) showed that copper and gold species are rather homogeneous distributed on the CeO$_2$ support. Although gold suffered leaching, copper and gold species did not agglomerate and thus, the deactivation of the catalyst might be attributed to the leaching of gold.

Conclusions

In this work, it is showed that cerium oxide supporting gold-copper species are highly active catalysts for converting glycerol to lactic acid at high reaction temperature and in aqueous basic medium. It is also showed that copper stabilized gold species supported on cerium oxide, allowing regenerating the catalyst for up to four catalytic cycles, while catalyst containing only gold deactivated after the first cycle. Interactions between Au and Cu are responsible for gold stabilization, allowing obtaining selective and stable gold catalysts at high reaction temperatures in aqueous medium. Further studies are needed to understand the process of deactivation of AuCu/CeO$_2$ catalysts.

Compliance with ethical standards

Conflict of interest   The authors declare that they have no conflict of interest.

References

Anand P, Saxena RK (2012) A comparative study of solvent-assisted pretreatment of biodiesel derived crude glycerol on growth and 1,3-propanediol production from Citrobacter freundii. New Biotechnol 29:199–205. https://doi.org/10.1016/j.nbt.2011.05.010

Auneau F, Noël S, Aubert G, Besson M, Djakovitch L, Pinel C (2011) On the role of the atmosphere in the catalytic glycerol transformation over iridium-based catalysts. Catal Commun 16:144–149. https://doi.org/10.1016/j.catcom.2011.09.011

Auneau F, Arani LS, Besson M, Djakovitch MC, Delbecq F, Sautet P, Pinel C (2012) Heterogeneous transformation of glycerol to lactic acid. Top Catal 55:474–479. https://doi.org/10.1007/s11244-012-9823-1

Behr A, Eilting J, Irawadi K, Leschinski J, Lindner F (2008) Improved utilisation of renewable resources: new important derivatives of glycerol. Green Chem 10:13–30. https://doi.org/10.1039/b710561d

Bozell JJ, Petersen GR (2010) Technology development for the production of biobased products from biorefinery carbohydrates-the US Department of Energy's "top 10" revisited. Green Chem 12:539–554. https://doi.org/10.1039/b922014c

Cargnello M, Gentilini C, Montini T, Fonda E, Mehraeen S, Chi M, Herrera-Collado M, Browning ND, Polizzi S, Pasquato L, Fornasiero P (2010) Active and stable embedded au@CeO$_2$ catalysts for preferential oxidation of CO. Chem Mater 22:4335–4345. https://doi.org/10.1021/cm101499x

Castillo Martinez FA, Balciunas EM, Salgado JM, Domínguez González JM, Converti A, Oliveira RPS (2013) Lactic acid properties, applications and production: a review. Trends Food Sci Technol 30:70–83. https://doi.org/10.1016/j.tifs.2012.11.007

Chang F-W, Ou T-C, Roselin LS, Chen W-S, Lai S-C, Wu H-M (2009) Production of hydrogen by partial oxidation of methanol over bimetallic Au–Cu/TiO$_2$–Fe$_2$O$_3$ catalysts. J Mol Catal A Chem 313:55–64. https://doi.org/10.1016/j.molcata.2009.08.002

Checa M, Auneau F, Hidalgo-Carrillo J, Marinas A, Marinas JM, Pinel C, Urbano FJ (2012) Catalytic transformation of glycerol on several metal systems supported on ZnO. Catal Today 196:91–100. https://doi.org/10.1016/j.cattod.2012.02.036

Datta R, Henry M (2006) Lactic acid: recent advances in products, processes and technologies - a review. J Chem Technol Biotechnol 81:1119–1129. https://doi.org/10.1002/jctb.1486

Della Pina C, Falletta E, Rossi M (2008) Highly selective oxidation of benzyl alcohol to benzaldehyde catalyzed by bimetallic gold–copper catalyst. J Catal 260:384–386. https://doi.org/10.1016/j.jcat.2008.10.003

Dodekatos G, Schünemann S, Tüysüz H (2018) Recent advances in thermo-, photo-, and electrocatalytic glycerol oxidation. ACS Catal 8:6301–6333. https://doi.org/10.1021/acscatal.8b01317

Dusselier M, Van Wouwe P, Dewaele A, Makshina E, Sels BF (2013) Lactic acid as a platform chemical in the biobased economy: the role of chemocatalysis. Energy Environ Sci 6:1415–1442. https://doi.org/10.1039/c3ee00069a

Fan Y, Zhou C, Zhu X (2009) Selective catalysis of lactic acid to produce commodity chemicals. Catal Rev 51:293–324. https://doi.org/10.1080/01614940903048513

Finn M, Ridenour JA, Heltzel J, Cahill C, Voutchkova-Kostal A (2018) Next-generation water-soluble homogeneous catalysts for conversion of glycerol to lactic acid. Organometallics 37:1400–1409. https://doi.org/10.1021/acs.organomet.8b00081

Ftouni J, Villandier N, Auneau F, Besson M, Djakovitch L, Pinel C (2015) From glycerol to lactic acid under inert conditions in the presence of platinum-based catalysts: the influence of support. Catal Today 257, Part 2:267–273 doi:https://doi.org/10.1016/j.cattod.2014.09.034, 257, 267, 273

Haruta M (1997) Size- and support-dependency in the catalysis of gold. Catal Today 36:153–166. https://doi.org/10.1016/S0920-5861(96)00208-8

Haruta M (2014) Chance and necessity: my encounter with gold catalysts. Angew Chem Int Ed 53:52–56. https://doi.org/10.1002/anie.201305987

Hisanori Kishida FJ, Zhouyu Zhou, Takehiko Moriya, and Heiji Enomotoy (2005) Conversion of glycerin into lactic acid by alkaline hydrothermal reaction. Chem Lett 34:2 doi:https://doi.org/10.1246/cl.2005.1560, 1560, 1561

Hutchings GJ, Haruta M (2005) A golden age of catalysis: a perspective. Appl Catal, A 291:2–5. https://doi.org/10.1016/j.apcata.2005.05.044

Jin X, Dang L, Lohrman J, Subramaniam B, Ren S, Chaudhari RV (2013) Lattice-matched bimetallic CuPd-graphene nanocatalysts for facile conversion of biomass-derived polyols to chemicals. ACS Nano 7:1309–1316. https://doi.org/10.1021/nn304820v

Johnson DT, Taconi KA (2007) The glycerin glut: options for the value-added conversion of crude glycerol resulting from biodiesel production. Environ Prog 26:338–348. https://doi.org/10.1002/ep.10225

Katryniok B, Paul S, Dumeignil F (2013) Recent developments in the field of catalytic dehydration of glycerol to acrolein. ACS Catal 3:1819–1834. https://doi.org/10.1021/cs400354p

Li Y, Nielsen M, Li B, Dixneuf PH, Junge H, Beller M (2015) Ruthenium-catalyzed hydrogen generation from glycerol and selective synthesis of lactic acid. Green Chem 17:193–198. https://doi.org/10.1039/c4gc01707b

Liu J, Zhao Z, Wang J, Xu C, Duan A, Jiang G, Yang Q (2008a) The highly active catalysts of nanometric CeO$_2$-supported cobalt oxides for soot combustion. Appl Catal, B 84:185–195. https://doi.org/10.1016/j.apcatb.2008.03.017

Liu X, Wang A, Wang X, Mou C-Y, Zhang T (2008b) Au-Cu alloy nanoparticles confined in SBA-15 as a highly efficient catalyst for CO oxidation. Chem Commun:3187–3189. https://doi.org/10.1039/b804362k

Liu B, Li C, Zhang Y, Liu Y, Hu W, Wang Q, Han L, Zhang J (2012) Investigation of catalytic mechanism of formaldehyde oxidation over three-dimensional ordered macroporous Au/CeO$_2$ catalyst. Appl Catal, B 111-112:467–475. https://doi.org/10.1016/j.apcatb.2011.10.036

Lu Z, Demianets I, Hamze R, Terrile NJ, Williams TJ (2016) A prolific catalyst for selective conversion of neat glycerol to lactic acid. ACS Catal 6:2014–2017. https://doi.org/10.1021/acscatal.5b02732

Ma L, Laasonen K, Akola J (2017) Catalytic activity of AuCu clusters on MgO(100): effect of alloy composition for CO oxidation. J Phys Chem C 121:10876–10886. https://doi.org/10.1021/acs.jpcc.6b12054

Mäki-Arvela P, Simakova IL, Salmi T, Murzin DY (2014) Production of lactic acid/lactates from biomass and their catalytic transformations to commodities. Chem Rev 114:1909–1971. https://doi.org/10.1021/cr400203v

Maris EP, Davis RJ (2007) Hydrogenolysis of glycerol over carbon-supported Ru and Pt catalysts. J Catal 249:328–337. https://doi.org/10.1016/j.jcat.2007.05.008

Maris EP, Ketchie WC, Murayama M, Davis RJ (2007) Glycerol hydrogenolysis on carbon-supported PtRu and AuRu bimetallic catalysts. J Catal 251:281–294. https://doi.org/10.1016/j.jcat.2007.08.007

Monteiro MR, Kugelmeier CL, Pinheiro RS, Batalha MO, da Silva César A (2018) Glycerol from biodiesel production: technological paths for sustainability. Renew Sust Energ Rev 88:109–122. https://doi.org/10.1016/j.rser.2018.02.019

Pagliaro M, Ciriminna R, Kimura H, Rossi M, Della Pina C (2007) From glycerol to value-added products. Angew Chem Int Ed 46:4434–4440. https://doi.org/10.1002/anie.200604694

Palacio R, Torres S, Lopez D, Hernandez D (2018a) Selective glycerol conversion to lactic acid on Co$_3$O$_4$/CeO$_2$ catalysts. Catal Today 302:196–202. https://doi.org/10.1016/j.cattod.2017.05.053

Palacio R, Torres S, Royer S, Mamede AS, Lopez D, Hernandez D (2018b) CuO/CeO$_2$ catalysts for glycerol selective conversion to lactic acid. Dalton Trans 47:4572–4582. https://doi.org/10.1039/c7dt04340f

Pereira CSM, Silva VMTM, Rodrigues AE (2011) Ethyl lactate as a solvent: properties, applications and production processes - a review. Green Chem 13:2658–2671. https://doi.org/10.1039/c1gc15523g

Prati L, Rossi M (1998) Gold on carbon as a new catalyst for selective liquid phase oxidation of diols. J Catal 176:552–560. https://doi.org/10.1006/jcat.1998.2078

Ramírez-López CA, Ochoa-Gómez JR, Fernández-Santos M, Gómez-Jiménez-Aberasturi O, Alonso-Vicario A, Torrecilla-Soria J (2010) Synthesis of lactic acid by alkaline hydrothermal conversion of glycerol at high glycerol concentration. Ind Eng Chem Res 49:6270–6278. https://doi.org/10.1021/ie1001586

Roy D, Subramaniam B, Chaudhari RV (2011) Cu-based catalysts show low temperature activity for glycerol conversion to lactic acid. ACS Catal 1:548–551. https://doi.org/10.1021/cs200080j

Sharninghausen LS, Campos J, Manas MG, Crabtree RH (2014) Efficient selective and atom economic catalytic conversion of glycerol to lactic acid. Nat Commun 5:5084. https://doi.org/10.1038/ncomms6084

Shen Z, Jin F, Zhang Y, Wu B, Kishita A, Tohji K, Kishida H (2009) Effect of alkaline catalysts on hydrothermal conversion of glycerin into lactic acid. Ind Eng Chem Res 48:8920–8925. https://doi.org/10.1021/ie900937d

Shen Y, Zhang S, Li H, Ren Y, Liu H (2010) Efficient synthesis of lactic acid by aerobic oxidation of glycerol on au–Pt/TiO_2 catalysts. Chem Eur J 16:7368–7371. https://doi.org/10.1002/chem.201000740

Shen L, Zhou X, Wang A, Yin H, Yin H, Cui W (2017) Hydrothermal conversion of high-concentrated glycerol to lactic acid catalyzed by bimetallic CuAux (x = 0.01–0.04) nanoparticles and their reaction kinetics. RSC Adv 7:30725–30739. https://doi.org/10.1039/c7ra04415a

Si R, Flytzani-Stephanopoulos M (2008) Shape and crystal-plane effects of nanoscale ceria on the activity of au-CeO_2 catalysts for the water–gas shift reaction. Angew Chem 120:2926–2929. https://doi.org/10.1002/ange.200705828

Sobczak I, Wolski Ł (2015) Au–Cu on Nb_2O_5 and Nb/MCF supports – surface properties and catalytic activity in glycerol and methanol oxidation. Catal Today 254:72–82. https://doi.org/10.1016/j.cattod.2014.10.051

ten Dam J, Kapteijn F, Djanashvili K, Hanefeld U (2011) Tuning selectivity of Pt/$CaCO_3$ in glycerol hydrogenolysis — a design of experiments approach. Catal Commun 13:1–5 doi. https://doi.org/10.1016/j.catcom.2011.06.007

Werpy T et al. (2004) Top Value Added Chemicals From Biomass, Results of Screening for Potential Candidates from Sugars and Synthesis Gas US Department of Energy 1000 Independence Ave, SW Washington, DC 20585, available at https://www.eereenergygov/biomass/pdfs/35523pdf 1. Accessed 11/01/2018

Wilson A, Bernard R, Boresztein Y, Croset B, Cruguel H, Vlad A, Coati A, Garreau Y, Prévot G (2015) Critical Au concentration for the stabilization of Au–Cu nanoparticles on rutile against dissociation under oxygen. J Phys Chem Lett 6:2050–2055. https://doi.org/10.1021/acs.jpclett.5b00791

Yang G-Y, Ke Y-H, Ren H-F, Liu C-L, Yang R-Z, Dong W-S (2016) The conversion of glycerol to lactic acid catalyzed by ZrO_2-supported CuO catalysts. Chem Eng J 283:759–767. https://doi.org/10.1016/j.cej.2015.08.027

Yin H, Zhang C, Yin H, Gao D, Shen L, Wang A (2016) Hydrothermal conversion of glycerol to lactic acid catalyzed by Cu/hydroxyapatite, Cu/MgO, and Cu/ZrO_2 and reaction kinetics. Chem Eng J 288:332–343. https://doi.org/10.1016/j.cej.2015.12.010

Zhang S, Li X-S, Chen B, Zhu X, Shi C, Zhu A-M (2014) CO oxidation activity at room temperature over Au/CeO_2 catalysts: disclosure of induction period and humidity effect. ACS Catal 4:3481–3489. https://doi.org/10.1021/cs500614f

Zhou C-H, Beltramini JN, Fan Y-X, Lu GQ (2008) Chemoselective catalytic conversion of glycerol as a biorenewable source to valuable commodity chemicals. Chem Soc Rev 37:527–549. https://doi.org/10.1039/b707343g

Zope BN, Hibbitts DD, Neurock M, Davis RJ (2010) Reactivity of the gold/water interface during selective oxidation catalysis. Science 330:74–78. https://doi.org/10.1126/science.1195055